MATERIALS PHYSICS AND MECHANICS RESEARCH ARTICLE

Submitted: October 17, 2024 **Revised: November 5, 2024** **Accepted: December 6, 2024**

Formation of liquid-like inclusions near pores in amorphous intercrystalline layers in high-temperature ceramics

M.Yu. Gutkin, S.A. Krasnitckii, N.V. Skiba ✉

Institute for Problems in Mechanical Engineering Russian Academy of Sciences, St. Petersburg, Russia

✉ nikolay.skiba@gmail.com

ABSTRACT

A theoretical model is suggested that describes a mechanism of plastic deformation in high-temperature ceramic materials containing amorphous intercrystalline layers (AILs) and pores in triple junctions of AILs. Within the model, the plastic deformation is realized through the generation of liquid-like inclusions on pore surfaces and their subsequent propagation along the AILs. In the exemplary case of high-temperature α-Al_2O_3 ceramics with AILs, the dependences of the critical values of the external shear stress for the formation of a liquid-like inclusion on deformation temperature in a wide range of the deformation temperatures from 300 to 1500 K are calculated. It is shown that the critical stress for the nucleation of a liquid-like inclusion strongly depends on the deformation temperature and weakly depends on the pore size.

KEYWORDS

high-temperature ceramics • amorphous intercrystalline layers • liquid-liked inclusions • pores • deformation temperature

Acknowledgements. *This work was supported by the Russian Science Foundation (grant No. 23-19-00236).*

Citation: Gutkin MYu, Krasnitckii SA, Skiba NV. Formation of liquid-like inclusions near pores in amorphous intercrystalline layers in high-temperature ceramics. *Materials Physics and Mechanics*. 2024;52(6): 8–16. http://dx.doi.org/10.18149/MPM.5262024_2

Introduction

The unique mechanical properties of high-temperature ceramics, such as very high strength, hardness and wear resistance at elevated temperatures, make these materials extremely promising for practical use [1–3]. According to experiments [4–6] and computer modeling [7–10], these properties are largely determined by the state and behavior of intercrystallite boundaries. Typically, these intercrystallite boundaries are layers of amorphous material with covalent interatomic bonds. The outstanding mechanical properties of the ceramic composites with the amorphous intercrystalline layers (AILs) [11,12] has stimulated growing interest in this class of materials. However, the experimental investigations of the AIL evolution are extremely complicated and laborious due to their small size. A significant role is played by computer simulations [7–10] and analytical theoretical models [13–20].

In particular, Glezer and Pozdnyakov [13,14] proposed the concept of grain boundary microsliding (GBMS) modeling the GBMS region as an inclusion in the form of an oblate ellipsoid. Later, a number of works [8–10] appeared on computer modeling of the mechanisms of plastic behavior of the AILs in amorphous silicon as a typical amorphous covalent material. The authors of these works showed that the atomic structure of the amorphous silicon included liquid-like and solid-like regions. In this case, the area of the liquid-like phase increases with increasing mechanical load, which

indicates that the areas of the liquid-like phase are carriers of plastic deformation in the amorphous silicon.

With the help of the results of computer modeling [8–10], some theoretical models [17–20] were developed that describe micromechanisms of the formation of the liquid-like inclusions under the action of an external shear stress in the grain boundaries (GBs) between the adjacent triple junctions. In the framework of these theoretical models, the enhancement of the plastic deformation in the ceramic composites with AILs was realized due to the formation of the liquid-like inclusions near the triple junctions of the AILs [17], due to the nucleation of nanocracks on the liquid-like phase inclusions [18], due to the liquid-like inclusions overcoming the triple junctions of the AILs and the penetration into a neighboring AIL [19], and due to nucleation and the extension of the liquid-like inclusions in the AILs with the subsequent emission of lattice dislocations from the triple junctions of the AILs and the glide of these dislocations into the bulk of a neighboring grain [20]. In the models, the liquid-like inclusions and their elastic fields were modeled by gliding dislocation loops [17,18] and dislocation dipoles [19,20] with increasing Burgers vectors. It is worth noting that these models [17–20] considered the nucleation of the liquid-like inclusion at the triple junctions of the AILs that did not contain other defects.

However, it is well known that the most ceramic materials are characterized by high porosity, which significantly reduces their fracture toughness and ductility characteristics [21–25]. In these circumstances, it is important for the practical use to develop mechanisms for increasing the fracture toughness and the ductility of high-temperature ceramic composites with high porosity.

Thus, the main aim of this work is to develop a micromechanism of the enhancement of the plastic deformation in the high-temperature ceramics with AILs through the nucleation and the extension of the liquid-like inclusions near the triple junctions of the AILs containing pores.

Model

Consider a cylindrical pore of radius R_0 placed in an equilibrium triple-junction of GBs with amorphous structure in a ceramic sample of α-Al_2O_3. It is supposed that the stress disturbance in vicinity of the pore induced by the remote shear stress τ is responsible for the nucleation and the subsequent propagation of the liquid-like inclusion along the GB as it is shown in Fig. 1.

The analysis of critical conditions for the formation of the liquid-like nucleus can be provided in the framework of the quasi-equilibrium energetic approach. According to this approach, the energy change due to the formation of the liquid-like nucleus is determined as follows:

$$\Delta W = W_{st} + \Delta H - A, \quad (1)$$

where W_{st} is the strain energy of the liquid-like nucleus generated on the pore surface, ΔH is the enthalpy increment due to the transition from the liquid to the solid phase [20] and A is the work done by the external shear stress τ.

The analytical expression of the first term in Eq. (1) is derived in this study. In doing so, the plastic shear inherent to the liquid-like nucleus is modeled by the dipole of edge dislocations with the variable Burgers vectors $\pm\boldsymbol{s}$ ($\pm s$-dislocation dipole). Within the

model, the first dislocation is placed in the pore center while the second one is located at the distance L from the pore surface (see Fig. 1). The corresponding strain energy of this dipole can be determined as a virtual work done by its own stress field on the plastic sliding (see, for example [26]):

$$W_{st} = \frac{s}{2}\int_{R_0}^{R_0+L}[\sigma_{xy}^{(1)} + \sigma_{xy}^{(2)}]dx, \quad (2)$$

where $\sigma_{xy}^{(1)}$ and $\sigma_{xy}^{(2)}$ are the shear stresses of the dislocations forming the dipole (hereinafter the Cartesian coordinate system (x,y) with the origin in the pore center and the x-axis directed along the GB with the liquid-like nucleus is applied). Equation (2) can be rewritten in terms of the Airy stress functions so that:

$$W_{st} = \frac{s}{2}\left[\frac{\partial \chi_1}{\partial y} + \frac{\partial \chi_2}{\partial y}\right]_{x=R_0,\ y=0}^{x=R_0+L,\ y=0}, \quad (3)$$

where χ_1 and χ_2 are the Airy stress functions of the dislocations. It is worth noting that the Airy stress functions for linearly elastic and isotropic bodies containing dislocations are well-studied and widely referred in literature [27]. For instance, the Airy stress function of an edge dislocation symmetrically placed in the center of a cylindrical pore can be cast as:

$$\chi_1 = -\frac{sG}{2\pi(1-\nu)} y\left(\frac{1}{2}\frac{R_0^2}{r^2} + ln\, r\right), \quad (4)$$

where G and ν are the shear modulus and the Poisson ratio, respectively, r is the radial coordinate with respect to the pore center.

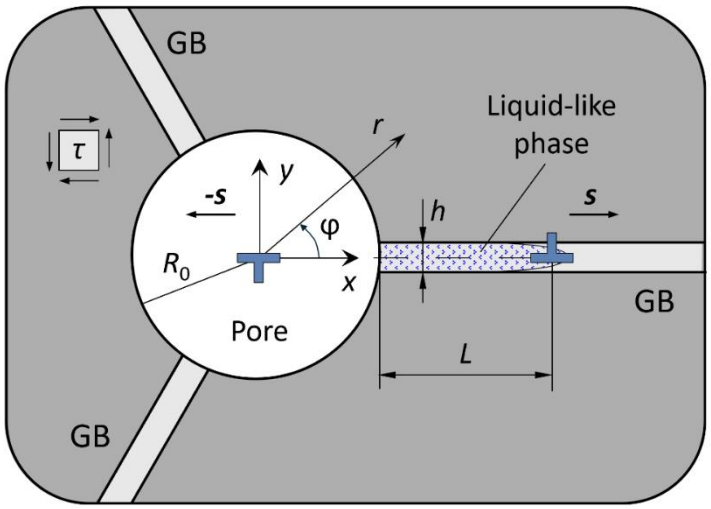

Fig. 1. A liquid-like inclusion emitted by the pore in a triple junction of the grain boundaries (GBs) under the external shear stress τ. The Cartesian (x, y) and polar (r, φ) coordinate systems associated with the pore center are shown

As for the dislocation located at a distance $d = R_0 + L$ from the pore center, the Airy stress function can be given by:

$$\chi_2 = \frac{sG}{2\pi(1-\nu)} y\left(\frac{1}{2}\frac{R_0^2}{r^2}\left(1 - \frac{r^2 r_1^2}{d^2 r_2^2}\right) + ln\frac{r r_1}{r_2}\right), \quad (5)$$

where the following denotations are introduced:

$$r_1 = \sqrt{r^2 + d^2 - 2rd\cos\varphi}, \quad (6)$$

$$r_2 = \sqrt{r^2 + (R_0{}^2/d)^2 - 2rR_0{}^2/d\cos\varphi}. \quad (7)$$

Subsisting Eqs. (4) and (5) in Eq. (3), one can finally obtain the analytical expression of the strain energy of the $\pm s$-dislocation dipole ejected by the cylindrical pore in the form:

$$W_{st} = \frac{Gs^2}{8\pi(1-\nu)}\left(-1 + 2\,ln\frac{L(2R_0+L)}{R_0 r_c}\right), \quad (8)$$

where r_c is the radius of the core of the second dislocation.

In further calculations, the parameter r_c is taken equal to the interatomic distance in α-Al_2O_3 ceramics: $a \approx 0.27$ nm [28]. It is worth mentioning that the effect of the decrease of the shear modulus G at elevated temperature can be incorporated into Eq. (8) by utilizing the experimental approximation for α-Al_2O_3 ceramic which is valid over a wide range of the temperatures [29]:

$$G(\text{GPa}) = 169 - 0.0229\,T, \quad (9)$$

where T is the temperature given in degrees Celsius. As for the Poisson ratio, it weakly depends on the temperature so that one can take $\nu = 0.23$.

Table 1. Temperature dependence of the specific enthalpy of α-Al_2O_3 ceramics

Temperature, K	300	400	500	600	700	800	900	1000	1100	1200	1300	1400	1500
Specific enthalpy of solid-like phase, kJ/mol	10.2	19.0	29.1	40.1	51.6	63.5	75.6	87.0	100.6	113.3	122.1	139.1	152.3
Increment of specific enthalpy from solid to liquid phase, kJ/mol	50.1	90.5	14.6	20.1	25.8	31.8	37.8	43.5	50.3	56.7	61.1	69.6	76.2

Turn now to the enthalpy term in Eq. (1). The experimental data on the enthalpy of solid-like phase H_m of α-Al_2O_3 ceramic are available in literature (see, for example, [30]), whereas the enthalpy of liquid-like phase H_i has not been thoroughly investigated. To avoid a lack of experimental research, one can estimate the unknown enthalpy of the liquid-like phase as $H_i \approx 1.5H_m$, whence for the increment of enthalpy due to the transition from solid to liquid phase is valid $\Delta H = H_i - H_m \approx 0.5H_m$. This approximation is in good agreement with experimental measures for Si ceramics in a wide range of temperatures [17]. The values of specific enthalpies of solid- and liquid-like phase, and increment of specific enthalpy in dependence of the temperature employed in the calculation below are given in Table 1. Finally, the enthalpy increment in Eq. (1) can be calculated in a similar way described in our previous work [20] with taking into account the data of Table 1 and the fact that the width of the liquid-like nucleus takes the average value $h \approx 4a$.

The last term in Eq. (1) is the work done by external forces on the formation of the liquid-like phase and can be defined as follows:

$$A = \tau\, s\, L. \quad (10)$$

Thus, all terms in Eq. (1) are defined. The section that follows moves on to the analysis of the energy change accompanying the formation of a liquid-like nucleus at the pore surface (Eq. (1)) under different temperature conditions.

Results

As mentioned above, the formation of the liquid-like inclusion is one of the effective mechanisms of plastic deformation in ceramics with the AILs such as α-Al_2O_3. Besides, it was noting that the porous structure of the sintered ceramics can significantly affect the initiation of the plastic deformation. In order to investigate the contribution of the latter factor to the nucleation of a liquid-like inclusion, the quasi-equilibrium energetic model is suggested.

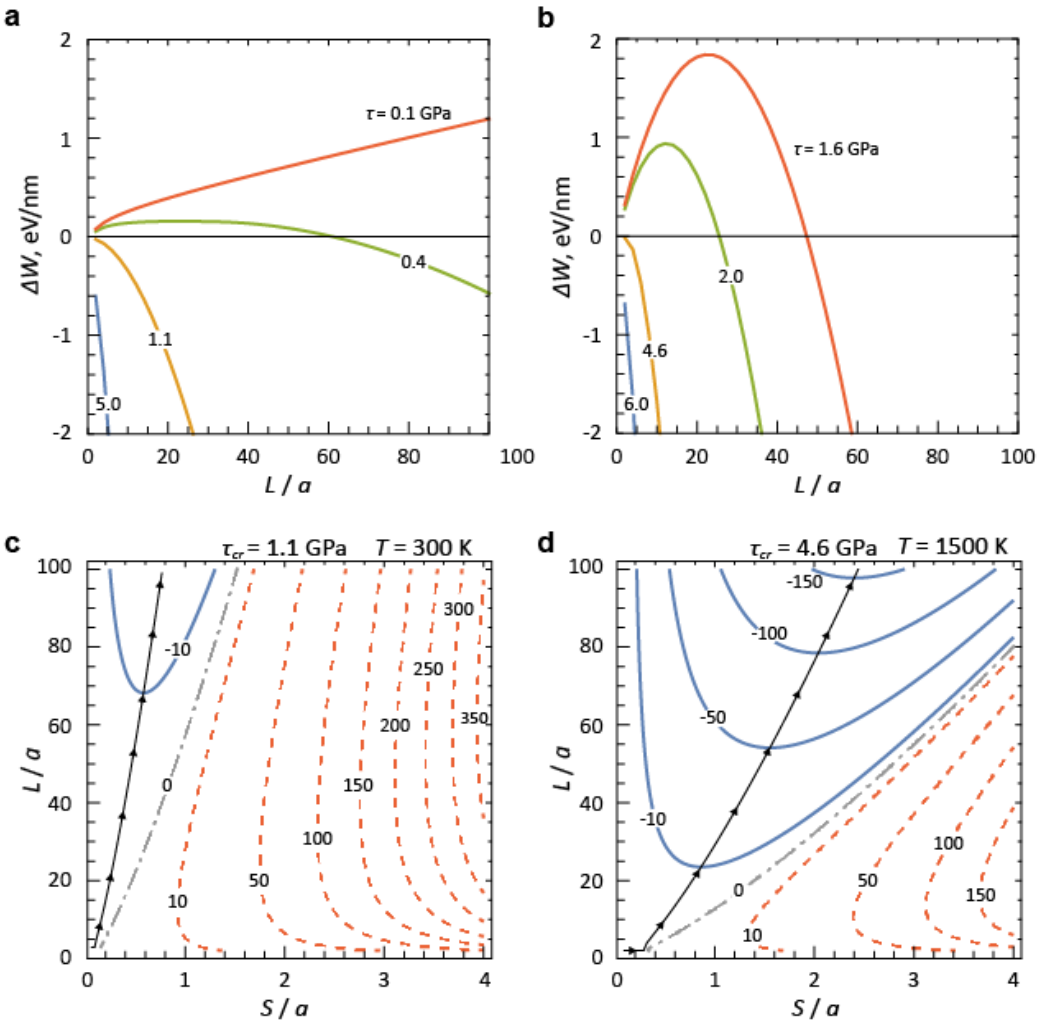

Fig. 2. The energy change accompanying the evolution of a liquid-like nucleous in vicinity of the pore of radius $R_0 = 100a$. The dependences of ΔW on the normalized length L/a are given for the plastic shear $s = 0.1a$ at different values of the remote stress τ for two temperatures: (a) $T = 300$ K and (b) $T = 1500$ K. Maps of ΔW in dependence on the normalized nucleus size L/a and its plastis shear s/a are given for two critical stress values: (c) $\tau_{cr}^{300\,\mathrm{K}} \approx 1.1$ GPa and (d) $\tau_{cr}^{1500\,\mathrm{K}} \approx 4.6$ GPa. The energy values on the maps are given in units of eV/nm for $\nu = 0.23$ and $a = 0.27$ nm

According to this model, the energy change due to the formation of the liquid-like nucleus at the cylindrical pore surface is determined by Eq. (1). Figures 2(a,b) illustrate the energy change $\Delta W(L)$ profiles obtained by Eq. (1) for quite low values of the plastic shear inherent to the liquid-like nucleus $s = 0.1a$. The curves $\Delta W(L)$ are given for pore size $R_0 = 100a$ and for different values of the remote shear stress τ in the cases of relatively

low temperatures (Fig. 2(a) for T = 300 K) and relatively high temperatures (Fig. 2(b) for T = 1500 K). As it is seen from the figures, the formation of the liquid-like inclusion is energetically favorable if the energy change becomes negative $W(L = 2a) < 0$ (hereinafter $L = 2a$ is taken as the smallest size of the nucleus). In other words, the shear stress τ should exceed some critical value τ_{cr} depending on the temperature conditions. For instance, the critical stress value $\tau_{cr} \approx 1.1$ GPa for T = 300 K, while $\tau_{cr} \approx 4.6$ GPa for T = 1500 K. It means that the formation of the liquid-like inclusion is inhibited at elevated temperatures. This fact can be elucidated by the intrinsic features of α-Al_2O_3 ceramic viz. The enthalpy contribution to the energy change of the process increases with the temperature growth.

The evolution of the liquid-like nucleus is demonstrated with the dependences of the energy change ΔW on the nucleus size L and its plastic shear s that are given for the critical stress values $\tau_{cr}^{300\,\mathrm{K}}$ and $\tau_{cr}^{1500\,\mathrm{K}}$ (see Fig. 2(c,d), respectively). The most preferable pathway of the nucleus evolution is depicted in the figures by the solid black line corresponding to the minimal values of the energy change starting from the initial values of parameters $L = 2a$ and $s = 0.1a$. What stands out from Figs. 2(c,d) is that, at the initial stage of the nucleus evolution, the nucleus has a tendency to accumulate the plastic shear until it reaches some value s_0 ($s_0 \approx 0.3a$ for T = 1500 K) conserving the size L=2a. At the next stage, the nucleus tends to evolve with increasing both the size L and the plastic shear s. It is worth mentioning that, at this stage, the size of the nucleus L almost linearly depends on the plastic shear s. The slope of these curves is strongly impacted by the temperature. For instance, for nucleus with $L = 100a$, the value of plastic shear is ~0.8a for T = 300 K while for T = 1500 K, the plastic shear is significantly bigger: ~2.4a. The slope value of the curve $L(s)$ is of great interest as an input for analyzing some more complicated mechanisms of the plastic deformation in ceramic materials such as the dislocation emission initiated by the liquid-like inclusion [20].

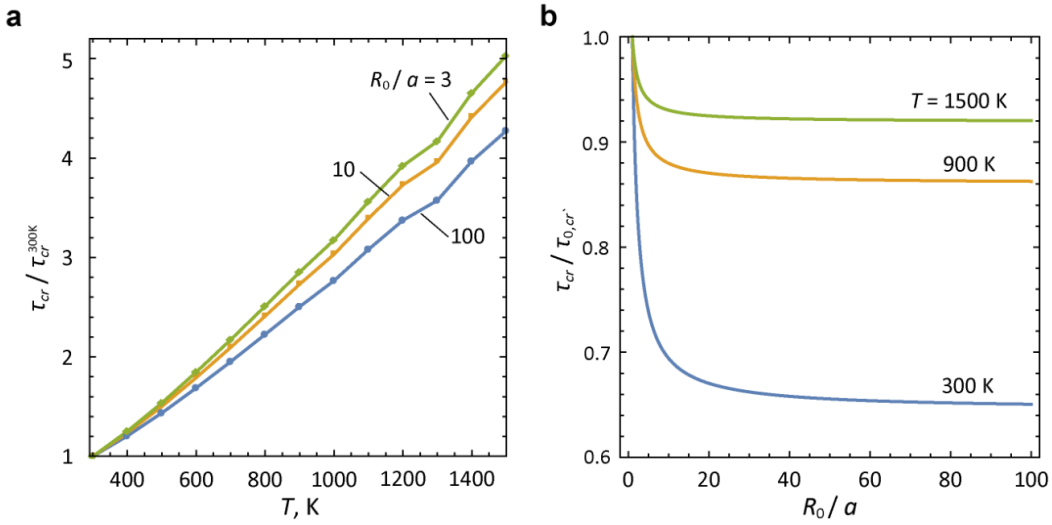

Fig. 3. The dependence of the critical stress τ_{cr} for the formation of a liquid-like nucleous on (a) the temperature T and (b) the pore radius R_0. The critical stress is given in units (a) of the critical stress $\tau_{cr}^{300\,\mathrm{K}}$ determined for different values of the pore radius $R_0 = 3a$, $10a$ and $100a$ and (b) of the critical stress $\tau_{0,cr}$ for the pore-free case obtained for different values of the temperature T = 300, 900 and 1500 K

The effect of temperature on the critical shear stress of the formation of liquid-like inclusion is demonstrated in Fig. 3(a). The figure shows the dependences of $\tau_{cr}(T)$ for different values of the pore radius $R_0 = 3a$, $10a$ and $100a$. As is seen from the plots, the critical stress gradually increases with the temperature growth. Hence, the nucleation of the liquid-like inclusions probably occurs at relatively low temperatures rather than at high temperatures. Besides, one can note that the effect of the pore facilitates the formation of the liquid-like nuclei i.e. the bigger the pore size, the lower the critical stress for the liquid-like nuclei formation.

Figure 3(b) illustrates the ratio of the critical stress τ_{cr} for the case with the pore to that one $\tau_{0,cr}$ for the case without pore in dependence of the normalized pore radius R_0/a for three different temperatures: $T = 300$, 900 and 1500 K. The plots sharply drop in the interval of relatively small R_0/a ($R_0/a < 15$) and then tend to some constant values for bigger R_0/a ($R_0/a > 15$). These constant values estimate the reduction of the critical stress in the case of relatively big pores ($R_0/a > 15$) under different temperature conditions. For instance, the reduction of the critical stress reaches ~8 % at elevated temperatures ($T = 1500$ K), ~14 % at relatively middle temperatures ($T = 900$ K) and ~35 % at low temperatures ($T = 300$ K). Thus, the temperature of deformation significantly affects the decline of the critical stress τ_{cr} viz. the lower the temperature the bigger the stress falling.

Conclusions

In summary, a theoretical model of a new micromechanism of the plastic deformation in the high-temperature ceramic composites with pores in triple junctions of amorphous intercrystalline layers (AILs) is developed. Within the model, the plastic deformation of a ceramic sample occurs through the emission of nuclei of the liquid-like phase from the triple junction of the AILs containing a pore under the action of the external shear stress. The energy characteristics of the generation of liquid-like phase nuclei at the AIL triple junctions containing pores are calculated. In the exemplary case of a high-temperature α-Al_2O_3 nanoceramics, the critical stresses for the formation of a liquid-like inclusion at the cylindrical pore in the AIL triple junction for wide temperature range are determined. The temperature dependences of these critical stresses are plotted for different sizes of the pore.

Thus, the model shows that the plastic deformation in high-temperature ceramic composites with pores in the triple junctions of the AILs can effectively occur through the generation of liquid-like inclusions on the pore surfaces and their propagation along the AILs, thereby increasing the crack resistance and plasticity of these composites.

In addition, this model can serve as an effective basis for comparative analysis of the possibility of the implementing other mechanisms of the plastic deformation enhancement and the fracture, such as the emission of the lattice dislocations from the triple junctions of the GBs containing pores and the generation of nanocracks on pores. The development of models describing the action of these alternative mechanisms of the plasticity and the fracture in the high-temperature ceramic composites is the subject of our future research.

References

1. Koch CC, Ovid'ko IA, Seal S, Veprek S. *Structural Nanocrystalline Materials: Fundamentals and Applications.* Cambridge: Campridge University Press; 2007.
2. Zhang D, Yu R, Feng X, Guo X, Yang Y, Xu X. Enhanced mechanical properties of Al_2O_3 nanoceramics via low temperature spark plasma sintering of amorphous powders. *Materials.* 2023;16(16): 5652.
3. Wang LY, An L, Zhao J, Shimai S, Mao XJ, Zhang J, Liu J, Wang SW. High-strength porous alumina ceramics prepared from stable wet foams. *J. Adv. Ceram.* 2021;10: 852–859.
4. Zhang ZL, Sigle W, Koch CT. Dynamic behavior of nanometer-scale amorphous intergranular film in silicon nitride by in situ high-resolution transmission electron microscopy. *Journal of the European Ceramic Society.* 2011;31(9): 1835–1840.
5. Subramaniam A, Koch CT, Cannon RM, Rühle M. Intergranular glassy films: An overview. *Materials Science and Engineering A.* 2006;422(1-2): 3–18.
6. Kleebe HJ. Structure and chemistry of interfaces in Si_3N_4 ceramics studied by transmission electron microscopy. *Journal of the Ceramic Society of Japan.* 1997;105(1222): 453–475.
7. Mo YF, Szlufarska I. Simultaneous enhancement of toughness, ductility, and strength of nanocrystalline ceramics at high strain-rates. *Applied Physics Letters.* 2007;90(18): 181926.
8. Demkowicz MJ, Argon AS. High-density liquidlike component facilitates plastic flow in a model amorphous silicon system. *Physical Review Letters.* 2004;93(2): 025505.
9. Demkowicz MJ, Argon AS. Liquidlike atomic environments act as plasticity carriers in amorphous silicon. *Physical Review B.* 2005;72(24): 245205.
10. Demkowicz MJ, Argon AS, Farkas D, Frary M. Simulation of plasticity in nanocrystalline silicon. *Philosophical Magazine.* 2007;87(28): 4253–4271.
11. Hulbert DM, Jiang D, Kuntz JD. A low-temperature high-strain-rate formable nanocrystalline superplastic ceramic. *Scripta Materialia.* 2007;56(12): 1103–1106.
12. Xu X, Nishimura T, Hirosaki N. Superplastic deformation of nano-sized silicon nitride ceramics. *Acta Materialia.* 2006;54(1): 255–262.
13. Glezer A, Pozdnyakov V. Structural mechanism of plastic deformation of nanomaterials with amorphous intergranular layers. *Nanostructured Materials.* 1995;6(5-8): 767–769.
14. Pozdnyakov VA, Glezer AM. Anomalies of Hall-Petch dependence for nanocrystalline materials. *Technical Physics Letters.* 1995;21(1): 31–36.
15. Bobylev SV, Gutkin MYu, Ovid'ko IA. Plastic deformation transfer through the amorphous intercrystallite phase in nanoceramics. *Physics of the Solid State.* 2008;50(10): 1888–1894.
16. Bobylev SV, Ovid'ko IA. Dislocation nucleation at amorphous intergrain boundaries in deformed nanoceramics. *Physics of the Solid State.* 2008;50(4): 642–648.
17. Gutkin MYu, Ovid'ko IA. A composite model of the plastic flow of amorphous covalent materials. *Physics of the Solid State.* 2010;52(1): 58–64.
18. Gutkin MYu, Ovid'ko IA. Plastic flow and fracture of amorphous intercrystalline layers in ceramic nanocomposites. *Physics of the Solid State.* 2010;52(4): 718–727.
19. Gutkin MYu, Mikaelyan K.N. A model of strain hardening in nanoceramics with amorphous intercrystalline layers. *Physics of Complex Systems.* 2021;2(2): 51-60.
20. Gutkin MYu, Skiba NV. Emission of lattice dislocations from triple junctions of grain boundaries in high-temperature ceramics with amorphous intercrystalline layers. *Materials Physics and Mechanics.* 2024;52(1): 39-48.
21. Liu J, Huo W, Zhang X, Ren B, Li Y, Zhang Z, Yang J. Optimal design on the high-temperature mechanical properties of porous alumina ceramics based on fractal dimension analysis. *Journal of Advanced Ceramics.* 2018;7(2): 89–98.
22. Ovid'ko IA, Sheinerman AG. Micromechanisms for improved fracture toughness in nanoceramics. *Reviews on Advanced Materials Science.* 2011;29(2): 105–125.
23. Vakaeva AB, Krasnitckii SA, Smirnov A, Grekov, MA, Gutkin MY. Stress concentration and distribution at triple junction pores of three-fold symmetry in ceramics. *Reviews on Advanced Materials Science.* 2018;57(1): 63-71.
24. Vakaeva AB, Krasnitckii SA, Grekov MA, Gutkin MYu. Stress field in ceramic material containing threefold symmetry inhomogeneity. *Journal of Materials Science.* 2020;55(22): 9311-9321.
25. Krasnitckii SA, Sheinerman AG, Gutkin MYu. Brittle vs ductile fracture behavior in ceramic materials at elevated temperature. *Materials Physics and Mechanics.* 2024:52(2): 82-89.
26. Mura T. *Micromechanics of defects in solids.* Netherland: Martinus Nijhoff Publishers;1987.

27. Eshelby JD. Boundary problems. In: Nabarro FRN. (ed.) *Dislocation in solids, Vol. 1*. Amsterdam: North-Holland Publishing Company; 1979. p.167–221.
28. Lagerlöf KPD, Heuer AH, Castaing J, Rivière JP, Mitchell TE. Slip and twinning in sapphire (α-Al2O3). *Journal of the American Ceramic Society*. 1994;77(2): 385–397.
29. Munro RG. Evaluated material properties for a sintered alpha-alumina. *Journal of the American Ceramic Society*. 1997;80(8): 1919-1928.
30. Archer DG. Thermodynamic properties of synthetic sapphire (α-Al2O3), standard reference material 720 and the effect of temperature-scale differences on thermodynamic properties. *Journal of Physical and Chemical Reference Data*. 1993;22(6): 1441–1453.

About Authors

Mikhail Yu. Gutkin
Doctor of Physical and Mathematical Sciences
Principal Researcher (Institute for Problems in Mechanical Engineering, Russian Academy of Sciences, St. Petersburg, Russia)

Stanislav A. Krasnitckii
Candidate of Physical and Mathematical Sciences
Researcher (Institute for Problems in Mechanical Engineering, Russian Academy of Sciences, St. Petersburg, Russia)

Nikolai V. Skiba
Doctor of Physical and Mathematical Sciences
Lead Researcher (Institute for Problems in Mechanical Engineering, Russian Academy of Sciences, St. Petersburg, Russia)